EDORIUM Journals

Edorium J Tumor Bio 2016;3:9–18.
www.edoriumjournaloftumorbiology.com

ORIGINAL ARTICLE PEER REVIEWED | OPEN ACCESS

Elevated PRP19 expression targets Bcl-2 and CASP3 expression to inhibit human lung adenocarcinoma cells apoptosis in vitro

Benjamin Arko-Boham, Isaac Okai, Shujuan Shao

ABSTRACT

Aims: The gene product of PRP19 besides constituting a central player in the spliceosomal machinery, functions in DNA damage repair, a process that aborts the hasty and unwarranted destruction of cell harbouring irreparable DNA damages by apoptosis. Such DNA alterations are common features underlying tumorigenesis. Based on our earlier report that PRP19 overexpression is inhibitory to proliferation in lung tumor cells, we further investigated the effect of elevated expression of PRP19 on cell survival. Methods: PRP19 expression was augmented in cultured A549 cells via plasmid transfection. Growing cells were subjected to various cell survival and apoptosis assays including CCK-8, DAPI, TUNEL and FITC-Annexin V staining. Lysates were obtained from harvested cells for immunoblotting for the assessment of expression of key apoptotic proteins. Results: Lung adenocarcinoma cells A549, overexpressing PRP19 via plasmid transfection exhibited delayed onset of apoptosis thereby prolonging their life span. Further test by western blot on key proteins involved in apoptosis regulation revealed that PRP19 overexpression led to augmented expression of anti-apoptotic Bcl-2 proteins while diminishing the expression of caspase-3. The expression of pro-apoptotic protein Bax, was unaltered among test and control groups. The Bcl-2 higher expression coupled with suppression of caspase-3 possibly underlies the in vitro inhibition of apoptosis following PRP19 upregulation. Conclusion: PRP19 overexpression resulted in a modest suppression of apoptosis to prevent the hasty destruction of cells with compromised genomic integrity. This is beneficial to the cell and may explain why PRP19 expression in tumor tissues is higher than in non-tumor tissues.

Keywords: Apoptosis, DNA damage, PRP19, Lung tumor

Benjamin Arko-Boham[1], Isaac Okai[2], Shujuan Shao[3]

Affiliation: [1]Department of Medical Laboratory Sciences, School of Biomedical and Allied Health Sciences, University of Ghana, Accra, Ghana; [2]Department of Human Anatomy, School of Medical Sciences, Kwame Nkrumah University of Science and Technology, Kumasi, Ghana; [3]Liaoning Provincial Key Laboratory for Proteomics, Department of Histology and Embryology, Dalian Medical University, 9 Western Section, Lvshun South Road, Dalian, China, 116044.

Corresponding Author: Benjamin Arko-Boham, P.O. Box KB 876, Korle-Bu, Accra, Ghana; Email: barko-boham@ug.edu.gh

Received: 13 April 2016
Accepted: 28 June 2016
Published: 07 July 2016

How to cite this article

Arko-Boham B, Okai I, Shao S. Elevated PRP19 expression targets Bcl-2 and CASP3 expression to inhibit human lung adenocarcinoma cells apoptosis in vitro. Edorium J Tumor Bio 2016;3:9–18.

Article ID: 100005T09BA2016

****

doi:10.5348/T09-2016-5-OA-2

INTRODUCTION

There are various forms of cancer with respect to the organs or tissues affected and have become a major clinical force battling humanity. Globally, the most common cancers diagnosed annually are those of the lungs, prostate, breast and cervix [1, 2]. Lung cancer accounts for the highest number of all annual global cancer-related deaths and remains the leading cause of death of all global cancer related mortalities. Lung cancer was responsible for approximately 1.8 million (12.9% of the total) new cancer cases and 1.6 million cancer-related deaths (19.4%) worldwide in the year 2012 alone [3–5]. This, undoubtedly, makes the disease a frightening case that needs more attention. The disease is characterized by uncontrolled cell growth within lung tissues. If untreated, cells may grow and spread to other parts of the body apart from the lungs which usually leads to death. In spite of improvements in diagnosis and treatment, a 5-year survival rate remains at an abysmal 13–15% [6, 7]. Adenocarcinoma, the most frequently diagnosed histological subtype accounts for about 40% of all lung cancer cases [3, 6, 8–11]. Biomarker identification for clinical use has been a major focus for biomedical research in the past decades. Although there has been significant advancement, a key setback to the discovery of new cancer biomarkers for effective clinical utilization in diagnosis and therapy remains the relatively non-specific nature of prospective biomarker candidates. This notwithstanding, several biomarkers for some cancers including lung cancer have been discovered and are currently clinically available [12, 13]. In view of this, there is need for more dedicated research aimed at discovering novel dependable and efficient cancer biomarkers for clinical utilization giving this work the needed impetuous.

We have earlier reported on the anti-proliferative effects of PRP19 overexpression in tumor cells [14] and now proceed to provide further evidence on repressive ability of the gene's amplification on apoptosis in lung tumor cells. The gene, with other names such as Pso4, PRP19 and NMP200 has the chromosomal location 11q12.2 and encodes for a 55-kDa protein with both cytoplasmic and nuclear presence [15–18]. The structure of the gene-product, according to Mahajan and Mitchell [16] is composed of an N-terminus, a C-terminus and an intervening homology domain. The N-terminus has a U-box with E3 ligase activity while the C-terminus is a tryptophan-aspartate 40 (WD-40) repeat domain for support and scaffolding [19]. Reports suggest the gene and its product to function in mRNA splicing, DNA damage repair, ubiquitination, oxidative stress response, transcription elongation and as a structural component of the nuclear membrane [17, 20–25].

Quantitative analyses of protein expression levels, as supported by a growing body of evidence, reveal that PRP19 is overexpressed in tissue samples of many human tumors compared to their non-tumor counterparts [17, 26]. It, however, remains unclear the underlying reason for the upregulation in the gene's expression in situ during tumorigenesis; as to whether it is of a direct and holistic beneficial value to the cells or a mere stress response mechanism that prompts the initiation of other vital reactions towards survival similar to that of p53 in response to genomic insults. Indeed, Dellago et al. [25] reported that PRP19 expression is increased in different cell types in response to oxidative stress. In vitro experimental evidences seem to suggest that PRP19 upregulation is profitable to cells owing to its known pro-survival properties. These pro-survival activities hinge on PRP19's DNA damage repair ability. Several reports indicate that upregulated PRP19 expression in vitro led to increased resistance to apoptosis and p53 phosphorylation, whereas cells with depleted PRP19 showed significantly diminished resistance to apoptosis which inadvertently resulted in truncated cellular life span [17]. It is therefore worthwhile, investigating the relevance of the observed alteration in the gene's expression in other cancers such as lung cancer in the attempt to decipher mechanisms underlying tumor development and progression which is vital to finding new cancer biomarkers.

MATERIALS AND METHODS

Selection of Cell line for in vitro Modeling

A range of lung cancer cell lines and one cervical cancer cell line were screened for PRP19 expression by western blotting. Whole cell lysates were extracted from cultured cells for western blotting. Since overexpression of the gene was intended, the cell line with the lowest PRP19 expression was selected as most suitable candidate for in vitro modeling. Cells used in the study were revived cells which had been stored (5–9 passages) in liquid nitrogen for four to six months. The cells had previously been received from the National Institute of Biologic Sciences (Beijing, China). The cell lines used were SPCA, A549, H446, H460, H520, 95C, 95D, HBE and Hela cells.

Cell Culture and Transfection Conditions

Cells were cultured in RPMI1640 culture medium (Gibco Life Technologies, China) supplemented with 10% fetal bovine serum (FBS) (Hyclone Thermo Scientific, China) without antibiotics and grown in a humidified incubator at 37°C and 5% CO_2 atmosphere. At between 80–90% confluence, cultures were detached using 0.1% trypsin and 0.02% EDTA for subculturing. For transfection, $6x10^3$ cells per well were plated in 24-well plates and allowed to grow to 60–70% confluence. A549-pEX-PRP19 and pEX-A549 cells were established by transfecting A549 cells with a pEX vector construct (Suzhou GenePharma, China) containing all regulatory elements using lipofectamine 2000 transfection reagent

(Invitrogen, USA) in accordance with manufacturer's instructions. Transfected cells were stably selected with 150 µg/ml geneticin (G418), (Gibco Life Technologies, Thailand) 24 hours post-transfection.

Whole Cell Lysates and Immunoblotting

Growing cells were harvested by trypsinization and pelleted by centrifugation and suspended in appropriate volumes of RIPA buffer (Beyotime, China) with 1% PSMF for protein extraction as directed by manufacturer. Between 150 and 300 µg of protein was separated by SDS polyacrylamide gel electrophoresis (SDS-PAGE) under denaturing conditions, blotted onto nitrocellulose membrane and blocked in 5% non-fat milk in 1X PBS for 1 hour. The membrane was incubated with the primary antibody at the appropriate dilution overnight at 4°C. Primary antibodies for PRP19 (Epitomics, USA) and all other proteins were diluted at 1:800 and 1:100 respectively. The antibodies used included polyclonal anti-caspase-3 (Abcam, UK), polyclonal anti-Bax (Proteintech, USA), polyclonal anti-NF-κB (Proteintech, USA), monoclonal anti-β-actin (Proteintech, USA), monoclonal anti-Bcl-2 (Thermoscientific, USA) and monoclonal anti-RB (Epitomics, USA). The secondary antibodies [goat-anti mouse and goat-anti rabbit (Thermoscientific, USA)] used were HRP coupled, diluted at 1:1000 and detected by chemiluminescence using ChemiDox™XRS+. β-actin was used as internal standard and normalizer.

4', 6-Diamidino-2-Phenylindole (DAPI) Staining

Growing cells were trypsinized and transferred into 96-well plates at a seeding density of 10^4 cells per well. Cell death was induced 24 hours post seeding with 30 µM cisplatin (Hansoh Pharmaceuticals Limited, China) for 0,24 and 48 hours for the different cell groups. Control groups received no cisplatin treatment. After the incubation period, cells were washed with 1 µg/ml DAPI (Roche, Germany) in methanol and then stained with the same concentration of DAPI-methanol solution for 15 minutes at 25°C in the dark after which cells were viewed under fluorescent microscope. Apoptosis-induced nuclear and cell membrane morphological changes were used to determine apoptosis. To estimate overall level of apoptosis within groups, cells in 10 randomly selected microscope fields (at x40) were counted. To calculate percentage apoptosis the ratio of apoptotic cells to total number of cells was multiplied by 100.

Terminal Deoxynucleotidyl Transferase dUTP Nick End Labeling (TUNEL) Assay

Growing cells were trypsinized, detached and transferred into 96-well plates at a seeding density of $1.5x10^4$ cells per well. Cell death was induced 12 hours post seeding with 30 µM cisplatin for 0, 24 and 48 hours for the different cell groups. Control groups received no cisplatin treatment. After cisplatin incubation period, cells were washed with 1X PBS and then covered with fixation solution (4% paraformaldehyde in PBS) for 1 hour at room temperature. Cells were rinsed with 1X PBS and subsequently covered with blocking solution (3% H_2O_2 in methanol) for 10 minutes at room temperature. Cells were again rinsed with 1X PBS and treated with permeabilization solution (0.1% Triton X-100 in 0.1% sodium citrate) for 5 minutes on ice. Cells were rinsed with 1X PBS, covered with 50 µl of TUNEL reaction mixture (Roche, Germany) and incubated for 1 hour at 37°C in darkness in a humidified atmosphere. Cells were finally rinsed 3 times with 1X PBS and visualized in a drop of 1X PBS under fluorescent microscope. TUNEL positive cells in 10 randomly selected microscope fields (at x40) were counted and their mean computed.

Fluorescein Isothiocyanate (FITC)-Annexin V Staining

Growing cells were treated with trypsin (without EDTA) and detached. Cells were washed with 1X PBS and collected by centrifugation at 2000 rpm for 5 minutes. The supernatant was removed and the pelleted cells resuspended in 500 µl of Annexin V binding buffer (Roche, Germany). Equal volumes (5 µl) of FITC solution and Propidium Iodide (PI) solution (Roche, Germany) were added to each cell suspension and incubated for 5 minutes at room temperature. Cells were then visualized and analyzed by FACS (BD Bioscience).

Stress Response Studies

Normal untransfected A549 cells growing under optimum conditions were introduced to different stress-inducing agents including; chemical (Geneticin) (Gibco, China), starvation and elevated temperature (heat shock at 42°C) for 2–3 hours. To serum starve the cells, healthily growing cells were incubated under optimum culture conditions for three hours with culture medium without FBS. For heat shock, healthily growing cells under optimum culture conditions were transferred into an incubator preheated to 42°C and incubated for 2 hours. In the chemical stress induction, growing cells were treated with growth medium (with FBS) containing 100 ug/ml geneticin (G418), (Gibco Life Technologies, Thailand) and incubated at optimum culture conditions for three hours. Cells were subsequently harvest and suspended in lysis buffer to obtain whole cell lysates for western blotting.

Statistical Analysis

The results presented are the mean and standard deviation of three independent experiments. Students' unpaired *t*-test was performed to compare groups using

SPSS 16 software. The p-values less than 0.05 were considered statistically significant.

RESULTS

A549 cells have lowest PRP19 expression among selected cell lines

To select an appropriate cell line for in vitro modeling, a range of lung cancer cell lines were screened for PRP19 expression. A549 cell line had the lowest PRP19 expression among the cell lines (Figure 1A) and was therefore selected as ideal candidate cell line for in vitro modeling since overexpression of the gene was intended. PRP19 expression in A549 cells was successfully augmented (Figure 1B-C) via plasmid transection

PRP19 overexpression impedes apoptosis

Results from all apoptotic assays suggested that PRP19 upregulation delayed the onset of apoptosis and significantly retarded its progress. In a DAPI experiment, which estimates the level of apoptosis by the degree of nuclear condensation or fragmentation, A549-pEX-PRP19 test group showed a lower rate of apoptosis compared to control groups at all experimental time points of 0, 24 and 48 hours (Table 1). At 24 hours post-cisplatin incubation, only a smaller population of the cells of the test group was in the Stage 1 (ring stage) of apoptosis while the larger population showed no visible sign of apoptosis. At the same time point control groups had larger populations of cells in both Stage 1 and Stage 2 (necklace stage) of apoptosis (Figure 2A–B). By 48 hours, an average of 76.6 ± 2.8% of cells of the control groups was in various stages of apoptosis with the predominant being Stage 2 and Stage 3 (nuclear collapse/disassembly stage) of apoptosis. The test group, however, registered 59.3 ± 2.1% of cell being apoptotic with a balanced distribution among Stage 1 and Stage 2 of apoptosis and a minimal number in Stage 3 of apoptosis (Figure 2A–B).

Similarly, a TUNEL assay produced results that conformed in trend with that of the DAPI experiment. A549-pEX-PRP19 cell group had reduced numbers of TUNEL positive (apoptotic) cells compared with control groups at various experimental time points (Figure 3 A–B). At the end of 48 hours of cisplatin treatment, control groups had an average of 84 ± 11 (SD) TUNEL positive cells per microscope field (taken at X40) as against that of 45 ± 8 (SD) TUNEL positive cells per microscope field for the test groups taken at the same magnification (Table 2) with *p*-value of <<0.001.

PRP19 Overexpression delays onset of Apoptosis

Subjected to FITC-Annexin V experimentation, it was evident that A549-pEX-PRP19 cells showed a delayed onset of apoptosis compared to cells of control groups. Following 24 hours of cisplatin treatment, just about 3% of the total cell population of the test group was found in the early stage of apoptosis compared to the over 8% of the cell population of control groups (Figure 4). After 48 hours of cisplatin treatment, total percentage apoptosis (early stage and late stage apoptosis) for the A549-pEX-PRP19, A549-pEX and A549 experimental groups were 11.62 ± 1.20%, 14.44 ± 0.94% and 19.43 ± 1.10%, respectively with a *p*-value of 0.035 (Table 3).

PRP19 overexpression amplifies Bcl-2 expression but diminishes CASP3 expression

A further test on some important proteins associated with and involved in apoptosis produced the following observation shown in Figure 5. Whereas the anti-apoptotic Bcl-2 showed elevated expression in A549-pEX-PRP19 cells compared to cells of control groups, the pro-apoptotic Bax had uniform expression among both test and control groups. The potent effecter protein of apoptosis, caspase-3 on the other hand, showed diminishing abundance in test groups cells compared with cells of control groups.

PRP19 expression is augmented under stress conditions

When A549 cells were subjected to various stress inducing conditions, augmentation of PRP19 expression was revealed by western blotting. Whole cell lysates from A549 cell groups subjected to 2 to 4 hours of starvation, heat shock at 42°C and geneticin treatment all showed comparable elevated levels of PRP19 expression (Figure 6A). Consequently, certain proteins that are known to be involved in the stress response pathway and cell cycle control were assayed for by western blotting. The results (Figure 6B) showed elevated expression of both retinoblastoma protein (RB) and NF-κB in test group cells compared to cells of control groups.

DISCUSSION

A pro-survival advantage PRP19 upregulation conferred on cells was delayed onset of apoptosis. In all apoptosis related assays conducted in this study, PRP19-overexpressing cells exhibited lowered rates of apoptosis compared to cells of control groups. In the DAPI experiment (Table 1 and Figure 2), over 52% of the cells in control groups were already in the Stage 2 (necklace stage) of apoptosis within 24 hours of cytotoxicity induction with cisplatin with an appreciable number already at the Stage 3 (nuclear collapse/disassembly stage) of apoptosis. Forty-eight hours post-cisplatin treatment, all cells in control groups showed visible signs of apoptosis and predominantly of the second and third stages. On the other hand, PRP19-overexpressing cells

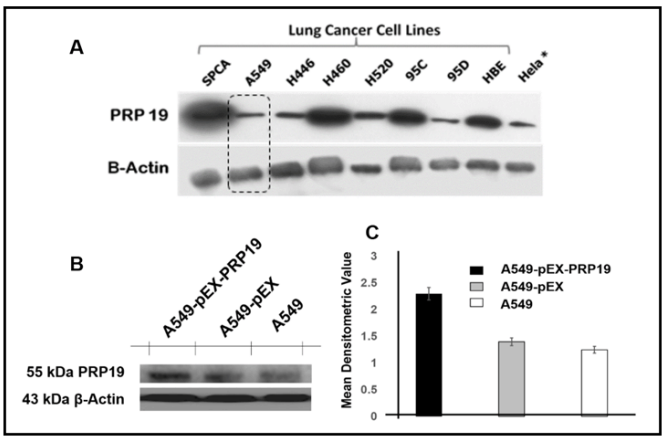

Figure 1: PRP19 expression among selected cell lines. (A) A549 cell line had the lowest PRP19 expression among the screened cell lines and was therefore selected as the most suitable candidate for in vitro modelling since overexpression of the gene was intended. * Cervical cancer cell line, (B, C) Western blot showing PRP19 upregulated expression in A549 cells post-transfection.

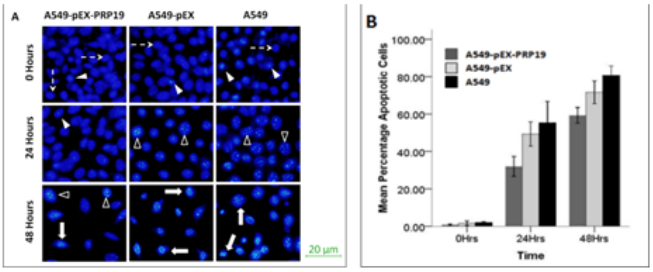

Figure 2: Estimation of Apoptosis with DAPI assay. (A) Representative micrographs of experimental groups at different experimental time points showing intact cell not undergoing apoptosis (thin broken arrows), cell at ring stage or stage 1 of apoptosis (block arrow heads), cells at the necklace stage or stage 2 of apoptosis (hollow arrow heads) and cells at the nuclear collapse/disassembly stage or stage 3 of apoptosis (thick solid arrows), (B) Graphical representation of percentage apoptotic cells of experimental groups at different experimental time points. The data are presented as the mean ± SE; n = 3.

Table 1: DAPI Assay Data Summary

Experimental Time Points	Mean Percentage ± SEM of Apoptotic Cells per Microscope Field (X40)			*p*-Value*
	A549-pEX-PRP19	A549-pEX	A549	
0 Hour	0.8 ± 0.2	1.6 ± 0.6	1.9 ± 1.2	0.27
24 Hour	32.0 ± 2.6	49.3 ± 3.2	55.3 ± 5.7	0.001
48 Hours	59.3 ± 2.1	71.6 ± 3.1	80.7 ± 2.5	<<0.001

* *p*-values were generated by comparing test group and control groups

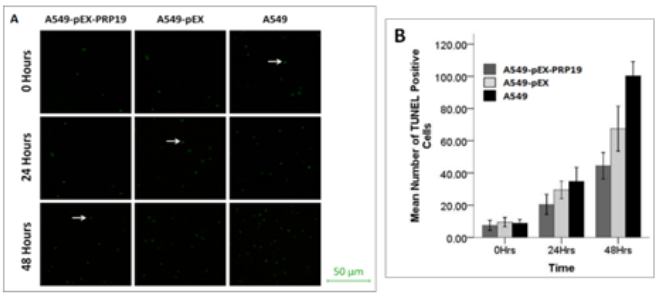

Figure 3: Estimation of Apoptosis with TUNEL assay. (A) Representative micrographs of experimental groups at different experimental time points. White arrows are pointing to nuclei of TUNEL positive cells, (B) Graphical representation of number of apoptotic cells of experimental groups at different experimental time points. The data are presented as the mean ± SD; n = 4.

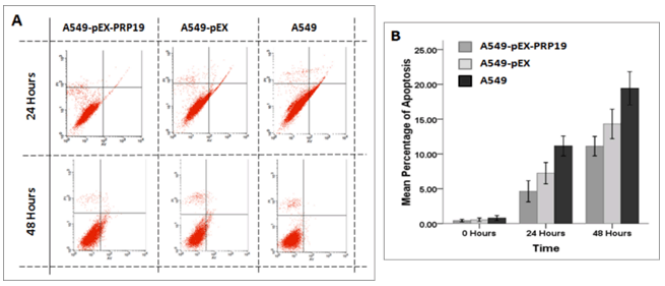

Figure 4: Estimation of Apoptosis with FITC-Annexin V assay. (A) Representative FACS analysis output of experimental groups at time 24 and 48 hours, (B) Graphical representation of number of apoptotic cells of experimental groups at different experimental time points. The data are presented as the mean ± SEM; n = 3.

at 48 hours of cytotoxic treatment had the predominant apoptotic cells at the second stage with a relatively low number at apoptosis stage 3. At hour 24 of treatment, only 32% of the cells showed visible signs of apoptosis and were largely of the stage 1 (the nuclear condensation stage). Microscopically, visible intracellular and nuclear morphology has been used to delineate apoptosis progression into three overlapping stages; Stage 1 (ring stage), Stage 2 (necklace stage) and Stage 3 (nuclear collapse/disassembly) [27]. In the test groups, entry

Table 2: TUNEL Assay Data Summary

Experimental Time Points	Mean Number ± SD of TUNEL Positive Cells per Microscope Field (X40)			*p*-Value*
	A549-pEX-PRP19	A549-pEX	A549	
0 Hour	8 ± 3	10 ± 3	9 ± 2	0.62
24 Hour	21 ± 6	30 ± 5	35 ± 4	0.045
48 Hour	45 ± 8	67 ± 13	100 ± 9	<<0.001

* *p*-values were generated by comparing test group and control groups

into Stage 1 was delayed and subsequent progression to the Stage 3 retarded compared to what was observed in control groups. It is therefore suggestive that PRP19 upregulation could be a chief contributor to the observed phenomenon.

Similar observations from other experiments corroborate the above finding. In the TUNEL experiments, there were less numbers of apoptotic cells in test group than in control groups at all the experimental time points (Table 2 and Figure 3) indicating upregulated PRP19's potency at counteracting the cytotoxic effects of cisplatin which lead to cell death by apoptosis. Results from the FITC-Annexin V experiments also supported the point that PRP19 upregulation delayed the onset of apoptosis when fewer cells of the test group were in early stage of apoptosis compared to control groups which had comparatively higher numbers (Table 3 and Figure 4) at the same experimental time points.

In a bid to gain more insight into the mechanism that underlies the above observation, the expression of certain proteins that are important players in apoptosis were assessed. Bax (Bcl-2-associated X protein), showed uniform expression among all groups (Figure 5) while the expression of Bcl-2 (B cell lymphoma 2) was elevated in cells of test group than those of control groups. Also, Caspase-3 expression was downregulated in cells of the test group than in their counterparts from the control groups. These findings were not unexpected looking at the functions of each of these proteins. Bax is a member of pro-apoptotic family of proteins which induce the opening of the mitochondrial voltage-dependent anion channels resulting in the release of cytochrome-c and other pro-apoptotic factors from the mitochondria, eventually leading to activation of caspases [28, 29]. They function as protagonist proteins of apoptosis to ensure that cells harboring unrepaired damages are quickly destroyed and eliminated. The uniform Bax expression among both test and control groups indicates that cells of all the groups

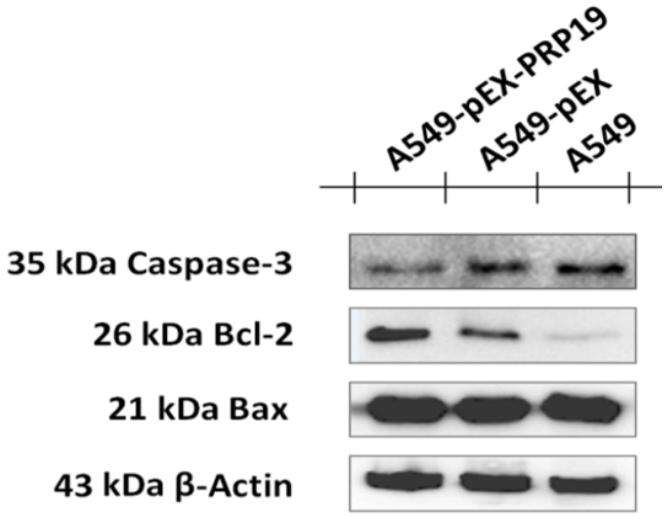

Figure 5: Western blotting results for some key proteins involved in apoptosis. CASP3 expression was lower in test groups than in control groups. Bcl-2 was highly expressed in test group cells than those of control groups whereas expression of Bax was unaffected among cells of both test and control groups. β-Actin was used as internal standard and normalizer.

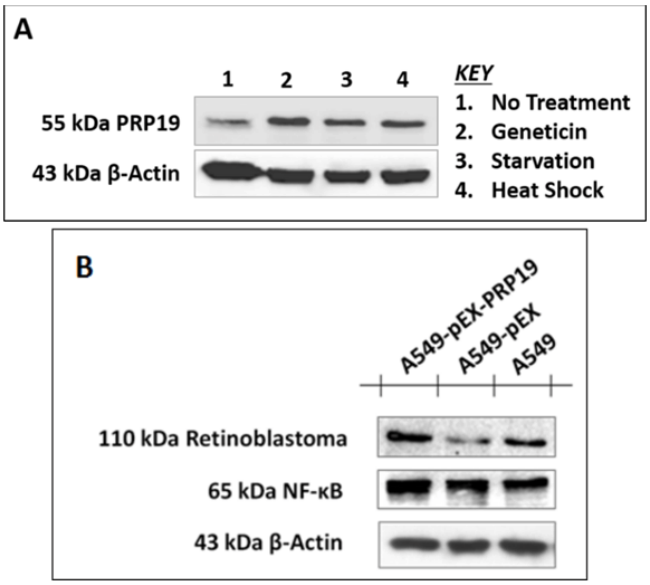

Figure 6: Western blotting results from stress response experiments. (A) Blots from whole cell lysates of A549 cells subjected to different stress-inducing conditions for 2 to 4 hours. All groups subjected to a form of stress showed elevated PRP19 expression on blots. (B) Blots for some key proteins involved in the stress response pathway (NF-κB) and cell cycle regulation (RB). The expression of both RB and NF-κB was upregulated in cells of test group than those of control groups. β-Actin was used as internal standard and normalizer.

Table 3: FITC-Annexin V Assay Data Summary

Experimental Time Points	Mean Percentage ± SEM of Apoptotic Cells			*p*-Value*
	A549-pEX-PRP19	A549-pEX	A549	
0 Hour	0.44 ± 0.09	0.54 ± 0.13	0.79 ± 0.18	0.311
24 Hour	4.63 ± 0.76	7.23 ± 0.77	11.15 ± 0.71	0.019
48 Hour	11.62 ± 1.20	14.44 ± 0.94	19.43 ± 1.10	0.035

* *p*-values were generated by comparing test group and control groups

were receiving equivalent degrees of cellular and genomic insults induced by cisplatin treatment. The difference, however, was the upregulated expression of Bcl-2 in the test group relative to controls. Bcl-2 is a member of the anti-apoptotic family of proteins which function to antagonize apoptosis. Bcl-2 in particular, functions specifically to inhibit the release of cytochrome-c, an important molecule for apoptosis initiation as part of the intrinsic apoptosis pathway [30–33].

Again, caspase-3 was of interest and the trend observed in its expression with PRP19 overexpression was intriguing. Caspase-3 is a major executioner protein (effector caspase) of apoptosis which is activated in apoptotic cells by both extrinsic (death ligand) and intrinsic (mitochondrial) pathways. It is present in cells as a zymogen and remains dormant until it is cleaved to activation by initiator caspases such as caspases 8 and 9 following initiation of apoptotic signaling events [34, 35]. Its expression positively associated with the degree of apoptosis among experimental groups. Control groups which had greater percentages of apoptosis equally had higher expression of caspase-3 as against the test group in which there was reduced rate of apoptosis. In brief, PRP19 overexpression led to augmented expression of anti-apoptotic proteins especially, Bcl-2 and diminished expression of caspase-3, the apoptosis effector enzyme. This ultimately resulted in a slowdown of the rate of apoptosis.

On stress response, the increase in PRP19 expression in response to different forms of stress suggests that the gene may be among the early acting genes in stress response. In stress response, the cell adopts multiple strategies to battle for survival against the offending agent. These strategies include cell cycle arrest that allows time for DNA damage repair in the cells. The observed elevated expression of retinoblastoma (RB) under stressing conditions (Figure 6B) therefore buttresses our earlier report where PRP19 overexpression promoted cell cycle arrest [14]. Members of the RB protein family function as molecular switch controlling G1 to S-phase transition serving as either transcription repressors or activators depending on their phosphorylation state [36]. When RB is hypophosphorylated it binds to E2F family of transcription factors and works as a transcriptional repressor. When adequately phosphorylated (by cyclin D and E), E2F dissociates from RB allowing it to transcribe genes necessary for DNA syntheses during the S-phase [37, 38].

Also, NF-κB is a protein complex that regulates DNA transcription, cytokine production and cell survival through its important role in cellular responses to stimuli including stresses [39]. In its inactive form, NF-κB has cytoplasmic location complexed with its repressor IκBα. When activated NF-κB is translocated into the nucleus where it binds to specific sequences of DNA response elements to set in motion a cascade of events that lead to transcription of downstream DNA and ultimately results in alteration of cell function [39–41]. The elevated NF-κB expression as observed in our work (Figure 6B) under stressing conditions therefore suggests attempts by the cells to survive the deleterious effects of the stress. Such survival attempts were enhanced by PRP19 overexpression since PRP19 overexpressing cell group had higher NF-κB expression under stress compared to control groups. More work however, needs to be done to elucidate the seeming PRP19-NF-κB pathway that is played out during cellular responses to stresses.

In summary, PRP19 overexpression conferred pro-survival advantages on cells which may underpin its upregulated expression in lung tumor tissues and other human tumors. PRP19 overexpression enhances cell survival by delaying the onset of apoptosis and retarded it progress. This is by means of PRP19's influence on some proteins involves in apoptosis. In particular, expression of anti-apoptotic genes is enhanced while that of apoptotic effector enzymes is inhibited. This inadvertently prevents the premature destruction of cells harbouring DNA damages in the bit to possibly achieve repair of the damages.

CONCLUSION

Overexpression of PRP19 resulted in a modest suppression of apoptosis to prevent the hasty destruction and removal of cells with compromised genomic integrity. The gene's expression in cells is upregulated in conditions that induce DNA damages. This may explain why its expression in tumor tissues is higher than in non-tumor tissues, an indication of accumulation of DNA damage which is quintessential of many cancers. In the light of intense search for cancer biomarkers for

early detection, prognosis and possible treatment, these findings hold great prospects. The relationship between PRP19 and human lung cancer is therefore worthy of further investigation.

****

Acknowledgements
We are thankful to Gong Linlin, Zhao Haoqi for their support and Mr Hui Wan for FACS analysis. Funding for this work was provided by: Mega-projects of National Science Research of China (973 Program, 2012CB967003), National Natural Science Foundation of China (81272225), 11 Doctoral Fund of the Ministry of Education of China (20132105110005), Education Department Foundation of Liaoning Province of China (L2013350).

Author Contributions
Benjamin Arko-Boham – Substantial contributions to conception and design, Acquisition of data, Analysis and interpretation of data, Drafting the article, Revising it critically for important intellectual content, Final approval of the version to be published
Isaac Okai – Acquisition of data, Analysis and interpretation of data, Drafting the article, Revising it critically for important intellectual content, Final approval of the version to be published
Shujuan Shao – Substantial contributions to conception and design, Revising it critically for important intellectual content, Final approval of the version to be published

Guarantor
The corresponding author is the guarantor of submission.

Conflict of Interest
Authors declare no conflict of interest.

REFERENCES

1. Danaei G, Vander Hoorn S, Lopez AD, et al. Causes of cancer in the world: comparative risk assessment of nine behavioural and environmental risk factors. Lancet 2005 Nov 19;366(9499):1784–93.
2. Lobo NA, Shimono Y, Qian D, Clarke MF. The biology of cancer stem cells. Annu Rev Cell Dev Biol 2007;23:675–99.
3. Ferlay J, Soerjomataram I, Dikshit R, et al. Cancer incidence and mortality worldwide: sources, methods and major patterns in GLOBOCAN 2012. Int J Cancer 2015 Mar 1;136(5):E359–86.
4. Ferlay J, Soerjomataram I, Ervik M, et al. GLOBOCAN 2012 v1.0, Cancer Incidence and Mortality Worldwide: IARC CancerBase No. 11 [Internet]. Lyon, France: International Agency for Research on Cancer; 2013. [Available at: http://globocan.iarc.fr]
5. Bray F. Transitions in human development and the global cancer burden. In: Wild CP, Stewart B eds. World cancer report 2014. Lyon: International Agency for Research on Cancer; 2014.
6. Borczuk AC, Gorenstein L, Walter KL, Assaad AA, Wang L, Powell CA. Non-small-cell lung cancer molecular signatures recapitulate lung developmental pathways. Am J Pathol 2003 Nov;163(5):1949–60.
7. Jemal A, Murray T, Samuels A, Ghafoor A, Ward E, Thun MJ. Cancer statistics, 2003. CA Cancer J Clin 2003 Jan-Feb;53(1):5–26.
8. Spiro SG, Silvestri GA. One hundred years of lung cancer. Am J Respir Crit Care Med 2005 Sep 1;172(5):523–9.
9. Ferlay J, Shin HR, Bray F, Forman D, Mathers C, Parkin DM. Estimates of worldwide burden of cancer in 2008: GLOBOCAN 2008. Int J Cancer 2010 Dec 15;127(12):2893–917.
10. Zochbauer-Muller S, Gazdar AF, Minna JD. Molecular pathogenesis of lung cancer. Annu Rev Physiol 2002;64:681–708.
11. Zu YF, Wang XC, Chen Y, et al. Thyroid transcription factor 1 represses the expression of Ki-67 and induces apoptosis in non-small cell lung cancer. Oncol Rep 2012 Nov;28(5):1544–50.
12. Molina R, Auge JM, Filella X, et al. Pro-gastrin-releasing peptide (proGRP) in patients with benign and malignant diseases: comparison with CEA, SCC, CYFRA 21-1 and NSE in patients with lung cancer. Anticancer Res 2005 May-Jun;25(3A):1773–8.
13. Boeck S, Wittwer C, Heinemann V, et al. Cytokeratin 19-fragments (CYFRA 21-1) as a novel serum biomarker for response and survival in patients with advanced pancreatic cancer. Br J Cancer 2013 Apr 30;108(8):1684–94.
14. Arko-Boham B, Xin Z, Okai I, et al. PRP19 upregulation inhibits cell proliferation in lung adenocarcinomas by p21-mediated induction of cell cycle arrest. Biomed Pharmacother 2014 May;68(4):463–70.
15. Gotzmann Jw, Gerner C, Meissner M, et al. hNMP 200: a novel human common nuclear matrix protein combining structural and regulatory functions. Exp Cell Res 2000 Nov 25;261(1):166–79.
16. Mahajan KN, Mitchell BS. Role of human Pso4 in mammalian DNA repair and association with terminal deoxynucleotidyl transferase. Proc Natl Acad Sci U S A 2003 Sep 16;100(19):10746–51.
17. Voglauer R, Chang MW, Dampier B, et al. SNEV overexpression extends the life span of human endothelial cells. Exp Cell Res 2006 Apr 1;312(6):746–59.

18. Fortschegger K, Wagner B, Voglauer R, Katinger H, Sibilia M, Grillari J. Early embryonic lethality of mice lacking the essential protein SNEV. Mol Cell Biol 2007 Apr;27(8):3123–30.
19. Vander Kooi CW, Ren L, Xu P, Ohi MD, Gould KL, Chazin WJ. The Prp19 WD40 domain contains a conserved protein interaction region essential for its function. Structure 2010 May 12;18(5):584–93.
20. Ohi MD, Vander Kooi CW, Rosenberg JA, et al. Structural and functional analysis of essential pre-mRNA splicing factor Prp19p. Mol Cell Biol 2005 Jan;25(1):451–60.
21. Urano Y, Iiduka M, Sugiyama A, et al. Involvement of the mouse Prp19 gene in neuronal/astroglial cell fate decisions. J Biol Chem 2006 Mar 17;281(11):7498–514.
22. Lu X, Legerski RJ. The Prp19/Pso4 core complex undergoes ubiquitylation and structural alterations in response to DNA damage. Biochem Biophys Res Commun 2007 Mar 23;354(4):968–74.
23. Song EJ, Werner SL, Neubauer J, et al. The Prp19 complex and the Usp4Sart3 deubiquitinating enzyme control reversible ubiquitination at the spliceosome. Genes Dev 2010 Jul 1;24(13):1434–47.
24. Chanarat S, Seizl M, Strässer K. The Prp19 complex is a novel transcription elongation factor required for TREX occupancy at transcribed genes. Genes Dev 2011 Jun 1;25(11):1147–58.
25. Dellago H, Khan A, Nussbacher M, et. al. ATM-dependent phosphorylation of SNEVhPrp19/hPso4 is involved in extending cellular life span and suppression of apoptosis. Aging (Albany NY) 2012 Apr;4(4):290–304.
26. Confalonieri S, Quarto M, Goisis G, et al. Alterations of ubiquitin ligases in human cancer and their association with the natural history of the tumor. Oncogene 2009 Aug 20;28(33):2959–68.
27. Toné S, Sugimoto K, Tanda K, et al. Three distinct stages of apoptotic nuclear condensation revealed by time-lapse imaging, biochemical and electron microscopy analysis of cell-free apoptosis. Exp Cell Res 2007 Oct 1;313(16):3635–44.
28. Shi Y, Chen J, Weng C, et al. Identification of the protein-protein contact site and interaction mode of human VDAC1 with Bcl-2 family proteins. Biochem Biophys Res Commun 2003 Jun 13;305(4):989–96.
29. Weng C, Li Y, Xu D, Shi Y, Tang H. Specific cleavage of Mcl-1 by caspase-3 in tumor necrosis factor-related apoptosis-inducing ligand (TRAIL)-induced apoptosis in Jurkat leukemia T cells. J Biol Chem 2005 Mar 18;280(11):10491–500.
30. Cleary ML, Smith SD, Sklar J. Cloning and structural analysis of cDNAs for bcl-2 and a hybrid bcl-2/immunoglobulin transcript resulting from the t(14;18) translocation. Cell 1986 Oct 10;47(1):19-28.
31. Gross A, McDonnell JM, Korsmeyer SJ. BCL-2 family members and the mitochondria in apoptosis. Genes Dev 1999 Aug 1;13(15):1899–911.
32. Komatsu K, Miyashita T, Hang H, et al. Human homologue of S. pombe Rad9 interacts with BCL-2/BCL-xL and promotes apoptosis. Nat Cell Biol 2000 Jan;2(1):1–6.
33. Yin J, Zhang YA, Liu TT, Zhu JM, Shen XZ. DNA damage induces down-regulation of Prp19 via impairing Prp19 stability in hepatocellular carcinoma cells. PLoS One 2014 Feb 28;9(2):e89976.
34. Porter AG, Jänicke RU. Emerging roles of caspase-3 in apoptosis. Cell Death Differ 1999 Feb;6(2):99–104.
35. Li P, Nijhawan D, Wang X. Mitochondrial activation of apoptosis. Cell 2004 Jan 23;116(2 Suppl):S57-9.
36. Baldi A, De Luca A, Esposito V, Campioni M, Spugnini EP, Citro G. Tumor suppressors and cell-cycle proteins in lung cancer. Patholog Res Int 2011;2011:605042.
37. Kaelin WG Jr. Functions of the retinoblastoma protein. Bioessays 1999 Nov;21(11):950–8.
38. Calbó J, Parreño M, Sotillo E, et al. G1 cyclin/cyclin-dependent kinase-coordinated phosphorylation of endogenous pocket proteins differentially regulates their interactions with E2F4 and E2F1 and gene expression. J Biol Chem 2002 Dec 27;277(52):50263–74.
39. Perkins ND. Integrating cell-signalling pathways with NF-kappaB and IKK function. Nat Rev Mol Cell Biol 2007 Jan;8(1):49–62.
40. Karin M, Ben-Neriah Y. Phosphorylation meets ubiquitination: the control of NF-[kappa]B activity. Annu Rev Immunol 2000;18:621–63.
41. Senftleben U, Cao Y, Xiao G, et al. Activation by IKKalpha of a second, evolutionary conserved, NF-kappa B signaling pathway. Science 2001 Aug 24;293(5534):1495–9.

SUGGESTED READING

- Zhou Z, Licklider LJ, Gygi SO, Reed R. Comprehensive proteomic analysis of the human spliceosome. Nature 2002;419:182–5.
- Yatabe Y. EGFR mutations and the terminal respiratory unit. Cancer Metastasis Rev 2010;29: 23–36.
- Zhang M-F, Zhang Z-Y, Fu J, Yang Y-F, Yun J-P. Correlation between expression of p53, p21/WAF1, and MDM2 proteins and their prognostic significance in primary hepatocellular carcinoma. J Transl Med 2009;7(110). doi: 10.1186/1479-5876-7-110
- Wasswa-Kintu S, Gan W Q, Man SF, Pare PD, Sin DD (2005). Relationship between reduced forced expiratory volume in one second and the risk of lung cancer: a systematic review and meta-analysis. Thorax 2005;60:570–5.
- Shimosato Y. Histological Typing of Lung and Pleural Tumors, 3ed. Malignant epithelial tumors. Nihon Rinsho 1999;60 Suppl 5:123–31.
- Siegel R, Naishadham D, Jemal A. (2013). Cancer Statistics, 2013. CA Cancer J Clin 2013;63:11–30.